Research Article

For reprint orders, please contact: reprints@futuremedicine.com

Nanomedicine

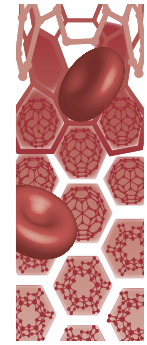

Artefactual nanoparticle activation of the inflammasome platform: *in vitro* evidence with a nano-formed calcium phosphate

Laetitia Pele*[,1], Carolin T Haas[1], Rachel Hewitt[1], Nuno Faria[1], Andy Brown[2] & Jonathan Powell[1]

[1]Medical Research Council – Human Nutrition Research, Elsie Widdowson Laboratory, Fulbourn Road, Cambridge, CB1 9NL, UK

[2]Institute for Materials Research, SPEME, University of Leeds, Leeds, LS2 9JT, UK

*Author for correspondence:
Tel.: +44 1223 426 356
Fax: +44 1223 437 515
laetitia.pele@mrc-hnr.cam.ac.uk

Aim: To determine whether *in vitro* experimental conditions dictate cellular activation of the inflammasome by apatitic calcium phosphate nanoparticles. **Material & methods**: The responses of blood-derived primary human cells to *in situ*-formed apatite were investigated under different experimental conditions to assess the effect of aseptic culture, cell rest and duration of particle exposure. Cell death and particle uptake were assessed, while IL-1β and caspase 1 responses, with and without lipopolysaccharide prestimulation, were evaluated as markers of inflammasome activation. **Results**: Under carefully addressed experimental conditions, apatitic nanoparticles did not induce cell death or engage the inflammasome platform, although both could be triggered through artefacts of experimentation. **Conclusion**: *In vitro* studies often predict that engineered nanoparticles, such as synthetic apatite, are candidates for inflammasome activation and, hence, are toxic. However, the experimental setting must be very carefully considered as it may promote false-positive outcomes.

Original submitted 13 September 2013; Revised submitted 6 March 2014

Keywords: apatite • caspase 1 • experimental conditions • IL-1β • inflammasome • nanoparticle

Human exposure to existing and novel nanostructures, or existing materials that have now been nano-engineered, is inevitable. A complete assessment of their interactions with the host must be addressed appropriately. It is well established that properties of the particles themselves (e.g., size, shape, aspect ratio, dispersion state and rate, composition, surface charge and solubility) and their interaction at the biological interface (e.g., formation of loose and hard protein corona, interaction with cell membrane) dictate how particles behave and how they are seen and handled by cells [1–3]. Nonetheless, despite this heterogeneity in the physico-chemical and biological properties of all that is termed 'nano', there are some properties that are more generally ascribed to nanoparticles than to their soluble or bulk counterparts [2]. One of these is an ability to activate the cellular inflammasome. In 2006, the late Jurg Tschopp and colleagues reported on the activation of the inflammasome by uric acid and calcium phosphate crystals [4]. Since then, numerous (engineered) nanoparticles have been attributed as inflammasome activators, including silica, titanium dioxide, aluminium hydroxide and calcium phosphates [5–10].

Both inflammasome and calcium phosphate are terms that encompass families. First the inflammasome: when caspase 1 is activated in a cell it has very specific targets. Pro-IL-18 and the more widely studied pro-IL-1β are cleaved to form the active, and mostly proinflammatory, cytokines (mature IL-18 and IL-1β). Canonical activation of caspase 1 is driven by the inflammasome platform following interactions of inflammasome sensor molecules (NOD-like receptors; NLRP and also the PYHIN family

Future Medicine part of fsg

protein AIM2) and the CARD-containing apoptosis-associated speck-like protein (ASC) [11,12]. Thus for IL-1β to be secreted by cells both the pro-cytokine must be transcribed and translated, and the inflammasome platform activated. Some molecules activate the inflammasome; some activate gene upregulation of the pro-cytokines and some do both [11,12]. Nanoparticles and especially nanominerals have acquired the reputation for inflammasome activation, sometimes concomitantly activating pro-IL-1β.

Second, the calcium phosphates: these vary in structure from fully amorphous calcium phosphate (ACP), with a primary grain size as small as 9 Å, to fully crystalline forms such as monetite, tricalcium phosphate and hydroxyapatite. Aside from ACP, all show a degree of crystallinity and, recently, the biologically relevant calcium phosphate family members have been comprehensibly reviewed by Dorozhkin [13]. Synthetic apatites that fairly closely correspond to biological apatite (i.e., bone mineral) are said to activate the inflammasome and induce IL-1β secretion by cells [14–17].

Most reports of nanoparticle-induced activation of the inflammasome have provided elegant detailed molecular biology-based studies characterizing the exact inflammasome platform and the various steps involved in activation. Less attention, however, has generally been paid to some basic but important particle and cell details. For example, what does the particle carry on its surface? What might it interact with in the cell culture medium? What is the importance of the cell activation status? When does particle uptake in culture exceed the *in vivo* situation where cells can migrate and be replaced by fresh ones? Here we have partly addressed these issues, focusing on apatitic nanoparticles, which we previously reported could induce cellular IL-1β secretion [17]. We chose not to undertake molecular studies of the inflammasome but, rather, to use IL-1β secretion, and in places caspase 1 secretion, as robust markers of inflammasome activation when experiments are carefully designed.

Material & methods

Assessment of *in vitro* particle formation & sizing

Preparation of calcium chloride solution

A stock solution of 40 mM calcium chloride ($CaCl_2$) was prepared by adding 0.58 g calcium chloride dihydrate (MW: 147.02 g/mol, AnalaR®; BDH, VWR International Ltd, Poole, UK) into 100 ml 0.9% sodium chloride solution (saline, Sigma-Aldrich, Poole, UK). After autoclaving, a 20 mM working solution was made up by diluting the stock solution 1:1 with saline.

In situ formation of calcium phosphate particles

In this protocol, for the formation of calcium phosphate particles *in situ* in a tissue culture medium (TCM), 4 mM (final concentration of additional Ca) $CaCl_2$ was added to supplemented TCM (namely RPMI 1640 which is naturally rich in phosphate, containing additionally 10% heat inactivated fetal calf serum [PAA], 2 mM L-glutamine [Sigma], 100 U/ml penicillin [Sigma] and 100 µg/ml streptomycin [Sigma]) [17]. As such, 250 µl of the calcium chloride solution were added to 1 ml supplemented TCM in 5 ml polystyrene round bottom tubes (Marathon Laboratory Supplies), yielding an additional concentration of 4 mM Ca^{2+} and hence precipitation of calcium phosphate particles that were characterized as below.

Particle sizing

To investigate the size distribution of calcium phosphate particles that formed in the supplemented TCM over 24 h, freshly prepared samples were analyzed by three independent methods; namely, nanoparticle tracking analysis (NTA), dynamic light scattering (DLS) and static light scattering (SLS), at time points 3, 8 and 24 h. Consistent with the manufacturers' guidelines, data for NTA, DLS and SLS are represented as particle number (10^6/ml), intensity (%) and volume frequency (%), respectively, as detailed below.

NTA

NTA was performed on a Nanosight NS500 (Nanosight, Amesbury, UK) using NTA2.3 Analytical Software. Particle suspensions were diluted eightfold (25-fold for time point 24 h) in supplemented TCM before samples were measured in technical triplicates for 60 s each and results were averaged. Two independent experiments were performed, each consisting of three replicate samples per time point. Data are shown as means of the six replicates (four replicates for time point 24 h).

DLS

DLS was performed on a Zetasizer Nano ZS (Malvern Instruments Limited, Malvern, UK) using Dispersion Technology Software 4.20. Triplicate measurements were taken from undiluted particle suspensions applying refractive indices of 1.63 for calcium phosphate particles and of 1.33 for the dispersant. Three replicate samples per time point were performed and data are shown as mean.

SLS

SLS was performed on a Mastersizer 2000 with a Hydro 2000µP Micro Precision sample dispersion unit (Malvern Instruments Limited). The measurement

procedure was adapted to enhance sensitivity and to preserve the experimental conditions under which the particles were formed. Baseline correction was carried out with fresh TCM. Subsequently, the dispersion unit was emptied and refilled with TCM alone or TCM with the additional 4 mM Ca^{2+} that had been incubated for 3, 8 or 24 h. The dispersion unit was run at 500 rpm and great care was taken to prevent the formation of bubbles. Three samples were collected for each time point and each sample was analyzed in triplicate (refractive index: 1.63; absorption 0.01).

Zeta-potential measurements

As an indicator of surface charge, zeta-potential measurements of particle suspensions were carried out, again at time points of 3, 8 and 24 h, by laser Doppler velocimetry on a Zetasizer Nano ZS (Malvern Instruments Limited). Electrophoretic mobilities of particles, in an applied electrical field of 8.16 V/cm (effective voltage of 49.8 V; electrode spacing 61 mm), were converted into zeta-potentials by Dispersion Technology Software 4.20 using Henry's equation and the Smochulowski approximation for aqueous media. The experiment was performed twice, each time with three replicate samples per time point. Data are shown as means of five (24 h) or six replicates (3 and 8 h) with the standard deviations reported.

Structural & chemical determination of *in vitro* precipitated particles

Following *in situ* formation of calcium phosphate particles for 24 h, the suspensions were drop cast onto holey carbon support films for transmission electron microscopy (Agar Scientific Ltd). The air-dried films were examined in a FEI CM200 field emission gun TEM operating at 197 kV fitted with an Oxford Instruments ultra thin window Si(Li) energy dispersive (EDX) spectrometer and a Gatan imaging filter (GIF 200; TEM images were analyzed using Gatan's Digital-Micrograph Software [version 3.11.2]).

The elemental content of particles was measured in the TEM by quantification of spot-energy dispersive x-ray (EDX) spectra; the Ca/P ratio was determined from the Oxford Instrument's ISIS processing software using virtual standards for Ca and P Kα x-ray peaks, monitored at a take-off angle of 20° and a specimen tilt angle of 15°. In addition to the above, dried calcium phosphate particles and control hydroxyapatite nanopowder (<200 nm; Sigma) were analyzed by FTIR. Spectra were collected using a Golden Gate single reflection diamond ATR accessory (Specac, Orpington, UK) with a Shimadzu IRPrestige-21 FTIR Spectrophotometer using the range 4000–750 cm^{-1} and 2 cm^{-1} resolution.

Cellular responses to the calcium phosphate particles: influence of experimental conditions

The study was approved by the research ethics committee of Cambridge (reference 03/296). For the purpose of the entire work, peripheral blood mononuclear cells (PBMC) were isolated from blood of recruited healthy volunteers, following informed consent, or purchased from the national blood service (NBS; Addenbrooke's Hospital site, Cambridge, UK). For each experimental condition investigated, we used blood cells from two to four different subjects unless otherwise stated. PBMC were isolated by density gradient centrifugation. Upon collection, 20–25 ml heparinized blood was mixed at a 1:1 ratio with HBSS (Sigma, UK). A total of 20–25 ml of the mixed solution was then carefully layered over 10 ml Lymphoprep (Axis-Shield, Norway) and centrifuged at 800 g at room temperature for 20 min. Separated mononuclear cells were then washed and resuspended at 1.10^6 cells/ml in TCM if used immediately or frozen for later use. Following cell stimulation, cell supernatants were collected after centrifugation at 1500 rpm for 5 min.

Effect of particle purity, cell status & duration of exposure

Here, we aimed to examine whether filtration of TCM and resting of cells prior to experimentation would impact on calcium phosphate nanoparticle formation and ensuing cellular responses. To that effect cells were: resuspended in 0.2 µm filtered or unfiltered TCM; were rested for 24 h at 37°C in 5% CO_2/95% air or used straight after isolation/thawing; and then stimulated with 250 µl 20 mM $CaCl_2$, in 5 ml polystyrene round bottom tubes. Following 24 h stimulation, supernatants were collected and stored at -70°C until analysis. Comparative responses were assessed by concomitantly challenging rested PBMC with $CaCl_2$ and the microbial-associated molecular pattern (MAMP) lipopolysaccharide (10 ng/ml LPS from *Escherichia coli*; Sigma).

To investigate the cellular responses to calcium phosphate particles over time, 1 ml cell suspensions (n = 2) were stimulated with 250 µl 20 mM $CaCl_2$ in the presence or absence of 10 ng/ml LPS (Sigma) or equivalent volume of vehicle (0.9% sodium chloride solution), after 24 h rest. Supernatants were then collected after 1, 3, 8 and 24 h incubation at 37°C in 5% CO_2/95% air and stored at -70°C until analysis.

Assessment of calcium phosphate toxicity

To explore the possible effects of calcium phosphate on cell death, rested PBMC (n = 2) were stimulated with the *in situ*-formed calcium phosphate nanoparticles or with equivalent volume of vehicle for 2–24 h at 37°C in 5% CO_2/95% air. After each time point, cells were

washed three-times in cold PBS at 400 g for 10 min at 4°C. Following the final wash, cells were re-suspended in 1x binding buffer (Invitrogen) at 1.10^6 cells/ml. A total of 100 µl cell suspension was then transferred to 5 ml polystyrene round bottom tubes where 5 µl annexin V and propidium iodide (PI; 250 ng/ml) were added. After gentle vortexing, the cells were left to incubate for 25 min in the dark at room temperature. Finally 400 µl of 1x binding buffer were added to each tube, and samples were analyzed by flow cytometry. Results are expressed as percentage of monocytes that stained positively for both PI and annexin V and referred to as percentage of dead monocytes.

Measurement of calcium phosphate uptake in CD14$^+$ cells by flow cytometry & flow imaging

To demonstrate the cellular uptake of calcium phosphate particles over time, fluorescent calcein (Sigma) was utilized to stain the calcium mineral particles as they formed and thus to identify particles subsequently taken up by phagocytic cells. 1 µl of 10 mg/ml calcein solution was added to the PBMC (1.10^6 cells/ml in TCM) prior to the experimental incubation with either vehicle or 250 µl 20 mM $CaCl_2$. Following incubation for 1, 3 or 24 h, cells were washed and stained with PerCP-Cy 5.5 CD14 antibody (BD Biosciences) for 20 min, as per manufacturer's protocol, and protected from light thereafter. After washing and fixing in 1% para-formaldehyde solution, samples were filtered, split and a minimum of 300,000 events per sample immediately acquired using a Cyan ADP flow cytometer (Beckman Coulter) with Summit software for acquisition and analysis. Remaining cells (a minimum of 10,000 events) were acquired using the ImagestreamX, INSPIRE and IDEAS acquisition and analysis software (Merck Millipore Amnis). For each instrument, appropriate unstained and single-stained compensation controls were run alongside.

Cellular responses to calcium phosphate particles using optimized experimental conditions

To dissect out further the potential involvement of calcium phosphate particles on inflammasome activation, we applied the optimized experimental conditions to blood cells from four independent subjects. Since there is limited pro-IL-1β in resting cells, which needs to be induced via Toll-like receptor (TLR) signaling [18], isolated PBMC (1.10^6 cell/ml) were first subjected to LPS prestimulation (10 ng/ml for 3 h) and then challenged with peptidoglycan (Pg) both in a crude (*Staphylococcus aureus*) or soluble (*E. coli*) form (both at 10 µg/ml; Sigma and Invivogen, respectively) or with the *in situ* precipitated calcium phosphate particles. As positive controls of inflammasome platform activation, cells were also subjected to adenosine triphosphate (ATP, 1 mM) ± LPS (10 ng/ml; Sigma) and monosodium urate crystals (MSU, Caltag-Medsystems Limited; 100 µg/ml). All supernatants were collected following 3 h stimulation as well as after 21 h post-challenge.

Measurement of secreted cytokines & caspase 1

IL-1β and caspase 1 were measured by commercial ELISA development kits and ELISA Quantikine kits, respectively, following the manufacturer's protocol (R&D Systems).

Statistics

All data are expressed as mean ± SEM (unless otherwise stated) and were analyzed by two-way ANOVA tests followed by Bonferroni multiple comparisons, where appropriate. The level of significance was set at $p \leq 0.05$.

Results

Physicochemical characterization of *in situ*-formed calcium phosphate

The (nonprecipitating) formation of nanoparticles in (complex) tissue culture medium limits ready separation of the pure nanomaterial. Thus, determination of the *in situ*-formed calcium phosphate structure drew upon multiple imaging and analytical data, namely: morphology, particle size, Ca:P ratio by EDX, selected area diffraction and analysis. Comparisons were made with established literature data for calcium phosphates.

Addition of calcium chloride (+4 mM) to RPMI 1640, which is a phosphate-rich tissue culture medium (TCM), and subsequent incubation at 37°C in 5% CO_2/95% air, resulted in the formation of nanostructured particles of acicular morphology (Figure 1A–C). The primary particle size could be identified as 100–150 nm in images of agglomerated particles (resulting from drying the suspensions on TEM grids). Further internal nanostructure of aggregated ultrafine crystals of individual primary particles could be seen at higher magnification (Figure 1B & C & Supplementary Figure 1A; see online at www.futuremedicine.com/doi/suppl/10.2217/nnm.14.58). In suspension in TCM, particles were typically of 150–180 nm Z-average aquated size, as shown by three independent light scattering techniques, (Figure 1D–F, Table 1 & Supplementary Figure 1B) which, allowing for the hydration shell, is in the same size range to the nanoparticulate structures observed by TEM (Figure 1B). In TCM particle size distribution remained stable for 8 h but started to shift, marginally, towards large particle sizes by 24 h (Figure 1D–F & Table 1). Zeta-potential measures indicated net negative charge of the particles over 24 h in TCM (Table 1).

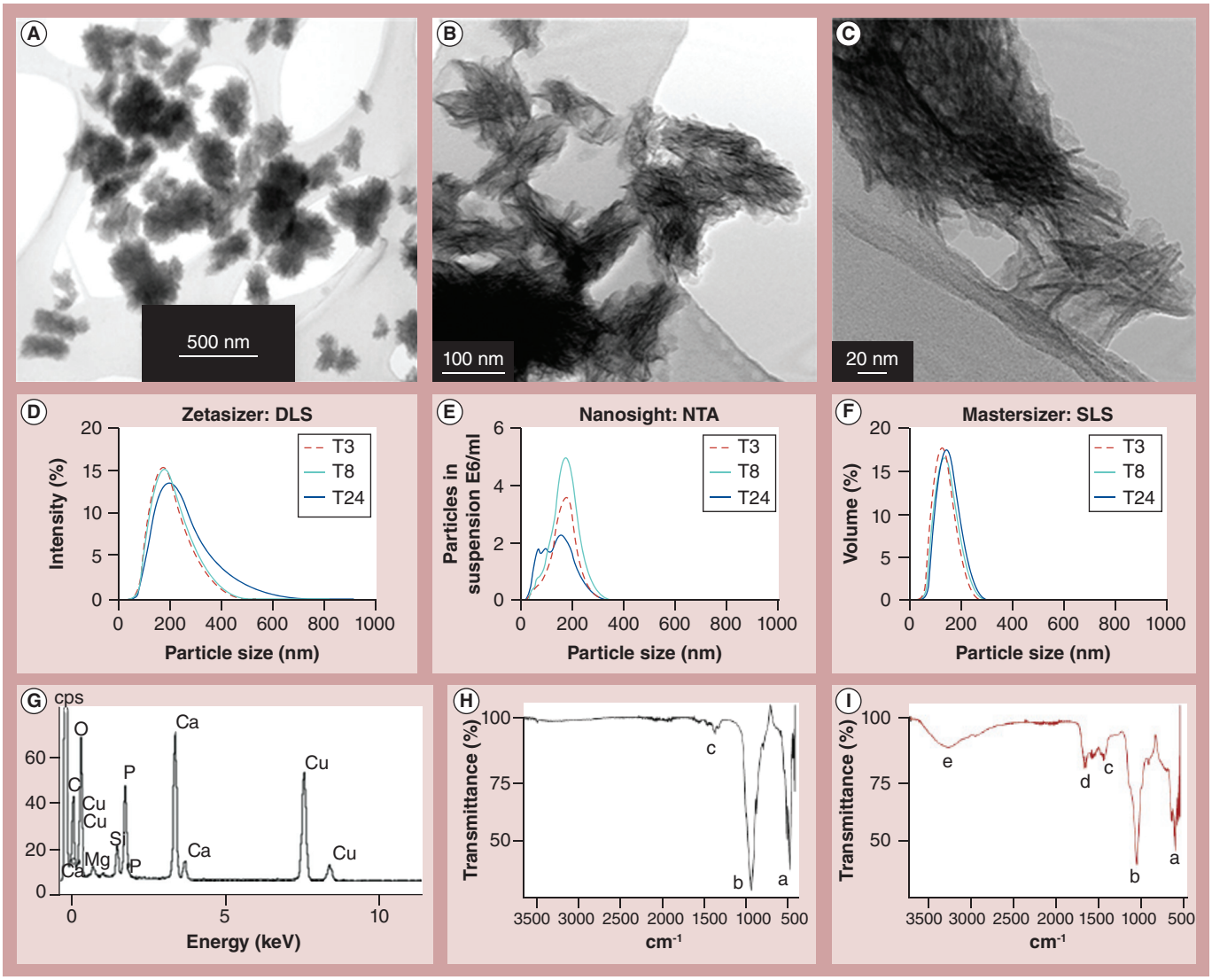

Figure 1. Physicochemical characterization of *in situ*-formed calcium phosphate nanoparticles. Following synthesis, calcium phosphate particles were analyzed **(A–C)** for particle size and structure by transmission electron microscopy, for size distribution in tissue culture medium by **(D)** DLS, **(E)** NTA and **(F)** static light scattering, and **(G)** for elemental composition by energy dispersive x-ray spectroscopy within the transmission electron microscopy (C and Cu signals are generated by the support film and grid). **(H)** Infrared analysis of hydroxyapatite standard (Sigma; 0–200-nm nanopowder) and **(I)** infrared analysis of the *in situ*-formed calcium phosphate particles in tissue culture medium with spectral features attributed as follows: **(a)** lattice vibrations, **(b)** phosphate vibration, **(c)** carbonate adsorption bands at 1465–1410 cm^{-1}, **(d)** amine adsorption bands from serum proteins at 1600–16,700 cm^{-1}, and **(e)** probable OH broadening from residual water with the main OH band at 3400 cm^{-1}.
DLS: Dynamic light scattering; NTA: Nanoparticle tracking analysis; SLS: Static light scattering; T3: 3 h; T8: 8 h; T24: 24 h.

TEM-EDX, acquired from particles suspended over holes in the support film, confirmed the particles to be calcium phosphate with an average Ca:P ratio of ~1.5 (Figure 1G), consistent with a nonstoichiometric apatite composition [13] that forms in serum-containing medium [19]. Selected area electron diffraction from these particles showed them to be polycrystalline having lattice spacings consistent with an apatite structure when the lattice spacings were matched to the strong reflections of the hydroxyapatite x-ray standard (Supplementary Figure 1A [inset] and Supplementary Table 1). Infrared analysis was consistent with hydroxyapatite (HA) cultured in TCM (Figure 1H & I) since amine adsorption bands from the serum proteins could be identified at 1600–1670 cm^{-1} [20], carbonate adsorption bands were present at 1465–1410 cm^{-1} and potential OH broadening from residual water with the main OH band were present at 3400 cm^{-1} [21]. The remaining bands at lower wavenumber (<1100 cm^{-1}) are due to lattice absorption and have previously been assigned to HA [22] since there are no other absorption bands for any

Table 1. Z-average, polydispersity indices and zeta-potential of apatitic particle suspensions at 3, 8 and 24 h.

Parameter	3 h	8 h	24 h
Z-average size (nm ± standard deviation)	152.0 ± 5.57	158.7 ± 16.80	181.2 ± 20.01
Polydispersity index (± standard deviation)	0.167 ± 0.02	0.156 ± 0.02	0.167 ± 0.04
Zeta-potential (mV ± standard deviation)	-14.48 ± 0.61	-14.06 ± 0.72	-13.73 ± 0.71

other calcium phosphate, such as dicalcium phosphate dihydrate and octacalcium phosphate, present in the current spectra [23].

Taken together our findings are consistent with the formation of polycrystalline nonstoichiometric apatite formed *in situ* in TCM which is retained upon drying. Rigorous identification of calcium-deficient hydroxyapatites (i.e., Ca:P ratios in the range 1.5–1.67) requires the use of several complementary characterization techniques and thermal treatment of powders [24]. We do not present powder XRD or thermal treatment results here; however, the morphology, composition and electron diffraction pattern of what we assume to be representative particles, plus the infrared fingerprint of the bulk material, do indeed invoke the formation of a nonstoichiometric apatite phase [20–22]. Since cells are exposed to the freshly formed hydrated species we use the terms 'apatite' and 'apatitic' throughout.

Innate cellular responses to the apatitic nanoparticles: influence of experimental conditions

Effect of resting of cells & TCM filtration

Having characterized the chemical and structural properties of the *in vitro*-precipitated calcium phosphate (apatite), we next investigated the cellular properties of these nanoparticles in the context of different experimental conditions. Cellular isolation is harsh and incurred stress lead to the release of endogenous danger signals (danger-activated molecular patterns) and activation of purinergic receptors, all of which contribute to inflammasome activation and consequent IL-1β production (so-called sterile inflammation) [25,26]. For example, if cells are stimulated with LPS then mature IL-1β is principally observed in freshly isolated monocytes rather than their 1-day rested counterparts [27–29]. Therefore, we first tested whether this also applied to primary human blood cells stimulated with the freshly formed apatitic nanoparticles. Unrested cells secreted a significant amount of IL-1β in response to challenge with the apatitic nanoparticles over 24 h when compared with unchallenged cells over the same time period (Figure 2A; $p < 0.05$). Resting cells prior to experimentation significantly reduced IL-1β secretion in response to apatite (Figure 2A). Addition of LPS, however, restored the IL-1β secretory effects of unrested cells (Figure 2A; $p < 0.05$).

Conventionally in cell culture experiments TCM would be filtered prior to use to help remove trace levels of macromolecular bacterial contaminants and serum complement aggregates that may occur during fetal calf serum heat treatment. Since the resting of cells reduced, but did not entirely abrogate, the IL-1β secretory response to apatitic nanoparticles (Figure 2A), we tested whether filtration of TCM prior to the addition of $CaCl_2$ (for *in situ* apatite nanoparticle formation) would further reduce IL-1β secretion. In nonrested cells there was no effect (Figure 2B) but in rested cells IL-1β secretion was reduced to background and could, again, be restored by the concomitant addition of LPS with the apatite nanoparticles (Figure 2B; $p < 0.001$).

Since IL-1β secretion in response to apatite stimulation in rested cells was greater when using unfiltered TCM (Figure 2A), we checked that apatite particles did not simply differ in physical characteristics due to their formation in 'different' media (i.e., changes in particle size distribution or charge inadvertently brought about by filtration of the TCM). DLS analysis and zeta-potential measures confirmed that filtration did not affect the physical characteristics of the formed particles (Supplementary Figure 2). Moreover the quantitative protein corona appeared to be the same (Supplementary Figure 2). We believe, therefore, that the difference is qualitative and reflects the ability of trace macromolecular pyrogens and/or serum protein aggregates to contribute to this corona. Indeed interaction of serum complement with nanoparticles can induce complement activation [30] and consequently inflammasome activation [31].

Taken together the above data suggest that under conditions that do not promote pro-IL-1β induction apatite does not induce significant secretion of mature IL-1β. From here onwards, therefore, experiments were carried out using filtered TCM and cells were challenged with apatite following 24 h rest.

Effect of duration of exposure to apatite on inflammasome activation

As noted above, failure to generate IL-1β does not mean failure to activate the inflammasome; the latter could occur but simply have no substrate to act on (i.e., pro-

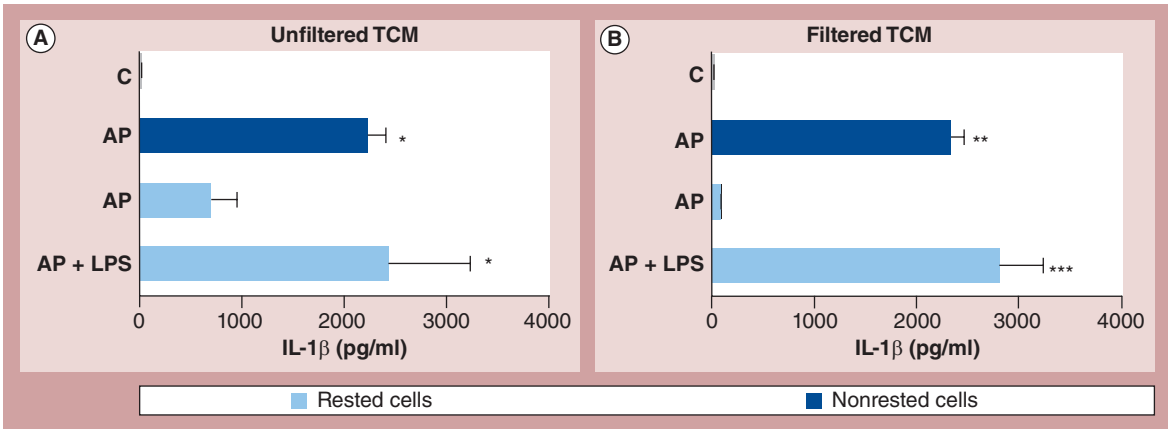

Figure 2. Influence of experimental conditions on IL-1β responses to apatitic nanoparticles. IL-1β secretion from peripheral blood mononuclear cells (1.10^6 cells/ml) in experiments that were carried out using **(A)** unfiltered TCM or **(B)** 0.2-μm filtered TCM . In each setting, peripheral blood mononuclear cells were either used immediately after isolation (dark blue) or rested for 24 h (light blue) and subsequently stimulated for 24 h with apatite nanoparticles that were formed *in situ* by addition of $CaCl_2$ to TCM, in the presence or absence of LPS (10 ng/ml) as indicated in the figure. Data are represented as mean ± standard error of the mean (n = 2).
*$p < 0.05$; **$p < 0.01$ and ***$p < 0.001$ versus control.
AP: Apatite; C: Control; LPS: Lipopolysaccharide; TCM: Tissue culture medium.

IL-1β). Inflammasome activation may be influenced by particle properties (e.g., shape, size and phase) and also by duration of exposure. To see whether the inflammasome was in fact activated by apatite and to relate this to duration of apatite exposure, we followed both caspase 1 and IL-1β secretion over the course of 24 h (in rested PBMC and using prefiltered TCM). Consistent with the findings above, apatite alone did not elicit IL-1β production (Figure 3A); however, it did induce caspase 1 secretion (Figure 3B; $p < 0.01$) showing that the inflammasome had been activated. Moreover IL-1β production was detectable when apatite was in the presence of LPS (to ensure that pro IL-1β was produced) commencing between 3–8 h stimulation and further increasing by 24 h (Figure 3B; $p < 0.0001$). Under these conditions, inflammasome activity was clearly induced by apatite.

Inflammasome activation by particles can be due to particle-induced reactive oxygen species and phagolysosomal destabilization [32–34] and, in some circumstances, lead to cell death. Incubation of mononuclear cells with apatite for long periods could therefore result in artefactual particle 'gorging', lysosomal disruption and cell death [2]. Indeed, in further studies we showed that apatite nanoparticles induced cell death between 6 and 12 h incubation (Figure 4; **$p < 0.01$), irrespective of the presence or absence of LPS (data not shown) and this mirrored the timing of caspase 1 secretion (Figure 3B).

Cellular responses to the apatitic nanoparticles in the absence of particle gorging

In light of the aforementioned results, cellular responses to apatite nanoparticles were re-addressed in a system that tried to avoid particle gorging (i.e., excessive particle loading). To confirm the extent of mononuclear cell uptake of apatite nanoparticles, by both flow cytometry and imagestream analysis, we utilized pure calcein, a widely used fluorescent probe for mineralized forms of calcium [35,36]. Unlike the calcein-acetomethoxy derivative (Calcein-AM), pure calcein is unable to passively enter cells to any significant extent and, therefore, the presence of this probe detected within cells relies upon both the binding of calcein to mineralized calcium formed in the media and the cellular uptake of this stained mineralized calcium. By incubating cells in media containing calcein with and without the addition of $CaCl_2$ (i.e., to form apatite *in situ* as above) we were able to control for even minor nonspecific uptake of this probe in the absence of apatite nanoparticles. Using this strategy, we showed that apatite nanoparticles were taken up as early as 1 h (Figure 5Ai), significant apatite loading of monocytes was achieved by 3 h (Figure 5Aii & B), and cells were gorged by 24 h exposure (Figure 5Aiii). These findings were confirmed by two independent techniques.

To re-test inflammasome activation without gorging, rested PBMC were first subjected to vehicle or LPS prestimulation to induce pro-IL-1β synthesis (at 0–3 h), washed and followed by a pulse with apatite for 3 h (from 3 to 6 h), washed again and chased for 21 h (from 6 to 24 h) with TCM only. Comparisons were made to cellular responses to soluble peptidoglycan (negative control; sPg), crude peptidoglycan (positive control, Pg) and to known inflammasome activators (i.e., ATP + LPS and MSU).

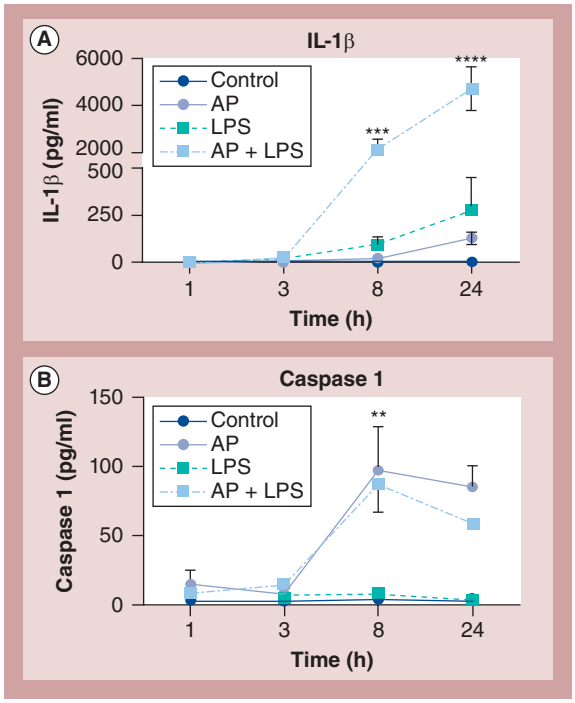

Figure 3. Influence of duration of exposure to apatitic nanoparticles on IL-1β and caspase 1 secretion in peripheral blood mononuclear cells. Time course measurement for **(A)** IL-1β and **(B)** caspase 1 secretion from rested peripheral blood mononuclear cells (1.10^6 cells/ml) following stimulation with LPS (10 ng/ml), apatitic nanoparticles in the presence or absence of 10 ng/ml LPS, or vehicle. Data are represented as mean ± standard error of the mean (n = 2, except at 8 h where n = 5).
*p < 0.05 (AP + LPS vs control); **p < 0.01 (AP vs control); ***p < 0.001; ****p < 0.0001 (AP + LPS vs control).
AP: Apatite; LPS: Lipopolysaccharide.

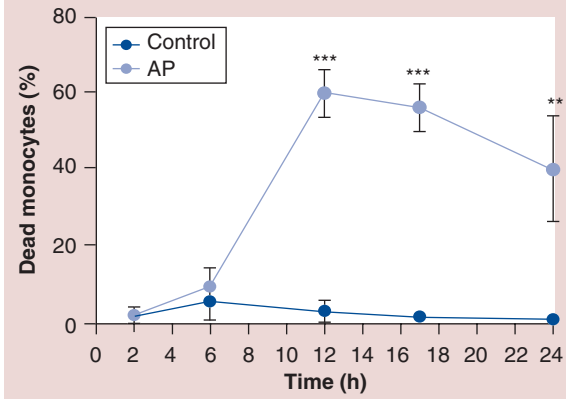

Figure 4. Apatitic nanoparticle-induced cytotoxicity. Flow cytometry measurement of cell death from the monocyte population within peripheral blood mononuclear cells (1.10^6 cells/ml) that were stimulated with apatite nanoparticles or vehicle over time. Data are represented as mean ± standard error of the mean (n = 2).
**p < 0.01; ***p < 0.001.
AP: Apatite.

Unlike the inflammasome activator, crude Pg, apatite failed to induce significant IL-1β versus vehicle control even when cells were primed with LPS (Figure 6A). Moreover, the response from apatite exposure was very similar to that of the negative control, namely soluble Pg from *E. coli*, which is not a significant activator of the inflammasome [37–39]. Unsurprisingly, without LPS priming, IL-1β secretion was also not observed in response to apatite nanoparticles although it was again observed for crude Pg and positive controls of the inflammasome platform (Figure 6B & Supplementary Figure 3).

Taken together, these data show that apatite nanoparticles neither activate the inflammasome nor induce the cellular IL-1β secretion to any extent, except as an artefact of experimentation.

Discussion

Nanoparticles, whether environmental [6,10], endogenously formed [7,8] or engineered for downstream applications [5,9] have been well studied and clearly linked to inflammasome activation. However, *in vitro* studies have on occasions been difficult to reconcile with *in vivo* situations [14,16,40], suggesting that applied *in vitro* experimental conditions do not always reflect *in vivo* outcomes. Here, our work demonstrates that the secretion of IL-1β and the activation of the inflammasome following *in vitro* cellular challenge with apatite nanoparticles depend upon experimental conditions.

Under aseptic conditions (to minimize the possibility of contaminants such as macromolecular MAMP or complement in the system) with nonactivated primary cells that were loaded but not gorged with apatite nanoparticles, we found no evidence of IL-1β secretion or inflammasome activation. The relevance of this to the *in vivo* situation should be carefully considered especially as, there, the source of nanoparticle exposure may be endogenous (i.e., of internal origin) or exogenous (i.e., of external origin). Endogenous particles such as bone apatite, or calcium phosphate derived from ectopic calcification, will be sterile (except during infection when the presence of nanoparticulates will not be the main concern). On the other hand, exogenous particles (e.g., dietary or environmental) are unlikely to be aseptic or, at least, unlikely to be devoid of surface adsorbed-molecules. However, during their initial *in vivo* transit, ostensibly through the lung or gastrointestinal tract, nanoparticle surfaces will interact with the myriad of molecules of endogenous biological fluids (e.g., salts, duodenal bile or lung surfactant protein, mucin, endogenous proteins, low molecular-weight ligands). Through substitution these are likely to strip exogenous particles

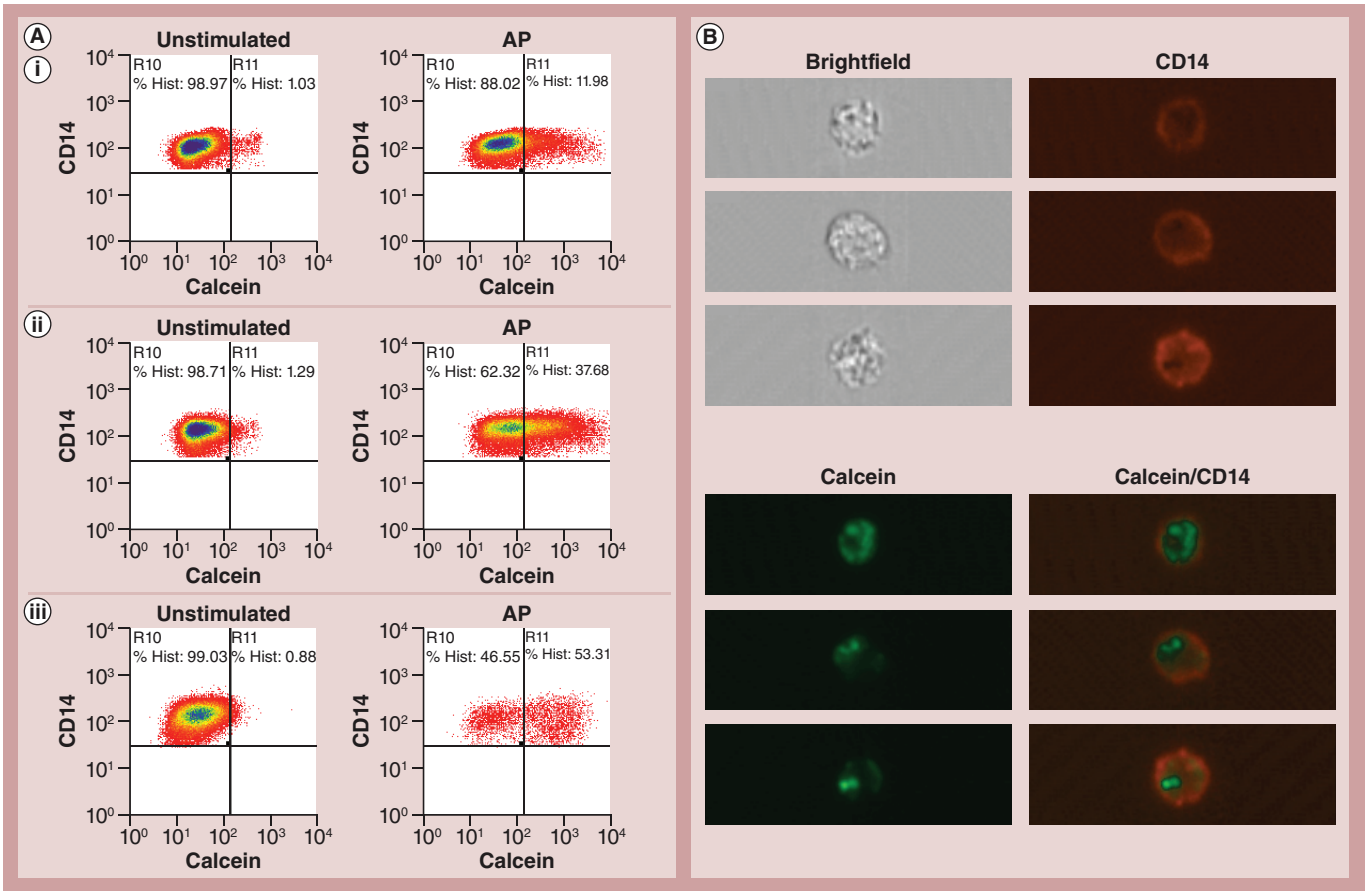

Figure 5. Apatitic nanoparticle uptake by monocytes. (A) Flow cytometric measurement in cells (CD14⁺ monocytes) that were stimulated with apatite or vehicle for **(i)** 1 h, **(ii)** 3 h and **(iii)** 24 h continuously. In each of the six panels only the viable CD14⁺ gated monocytes are imaged and thus occupy the top two quadrants. The colours represent density of cells in their plotted space (blue being the most dense and red the least). The right hand quadrants represent cells showing calcein positivity and thus intracellular calcium ('unstimulated') while the addition of apatite shows a marked and rapid increase in calcein positivity ('AP') and by 24 h few viable cells remain. **(B)** Imaging with a second independent technique, namely Image stream, showing three separate example images of CD14⁺ Calcein⁺ gated cells 3 h after challenge and showing internalization of AP particles.
AP: Apatite.

of any adsorbed, inflammasome-activating MAMPs and exchange them for more benign, self-recognized molecules. The exception is the distal gastrointestinal tract, where turnover of the commensal microbiota releases large quantities of MAMPs, such as LPS and peptidoglycan. However, intestinal cells are uniquely hyporesponsive (i.e., resistant) to inflammatory stimulation by MAMPs [41]. Thus, in our view, carefully characterized aseptic conditions are appropriate for the *in vitro* study of nanoparticles.

The choice of cells 'at rest' to represent the *in vivo* situation could also be debated. Inflammation, especially mildly so, is common place in the population. We used primary cells because immortal or transformed cells (i.e., cell lines) clearly undergo substantial changes compared with their *in vivo* counterparts. Nonetheless, primary cells are most commonly derived from blood and, thus, may undergo substantial stress during phlebotomy and isolation by density gradient centrifugation. However, in the experiments reported herein, even when we primed rested cells with LPS, which is a significant inflammatory stimulus, we still found no cause to suggest that apatitic nanoparticles stimulated IL-1β secretion or, therefore, activated the inflammasome.

In our opinion it is cellular gorging of nanoparticles that is most likely responsible for *in vitro* inflammasome activation and which commonly leads to misinformation between *in vitro* and *in vivo* exposure. Phagocytic cells are programmed to mop up particles from their environment. Unlike with *in vitro* cultures, *in vivo* cells may migrate and are readily replaced by freshly recruited cells. Moreover the epithelial barrier blocks most particle entry and ensures a rate of influx that is readily dealt with by underlying macrophages or immature dendritic cells. Even when

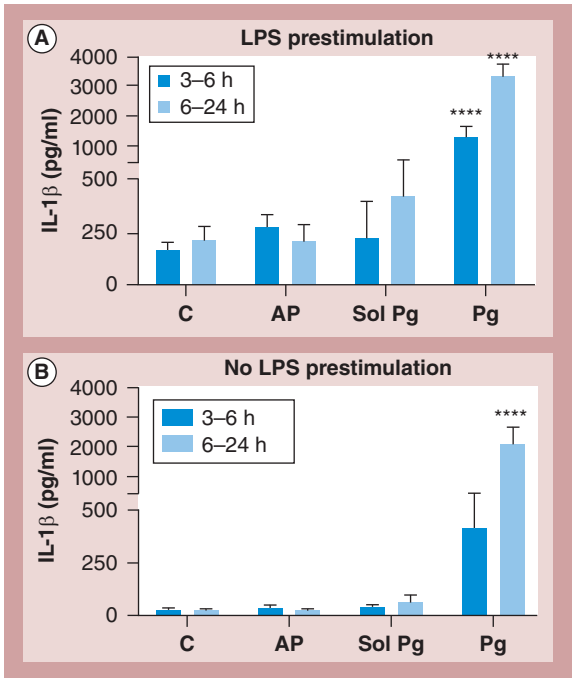

Figure 6. Optimized innate cellular responses to apatitic nanoparticles. IL-1β responses from peripheral blood mononuclear cells (1.10^6 cells/ml), **(A)** with or **(B)** without LPS prestimulation (3 h), and then challenged with vehicle, AP nanoparticles, soluble or crude peptidoglycan (Sol Pg and Pg, both at 10 μg/ml). IL-1β was measured after a further 3 h (i.e., between 3 and 6 h; dark blue) and 18 h after that (i.e., between 6–24 h; light blue). Data are represented as mean ± standard error of the mean (n = 4).
****$p < 0.0001$; ***$p < 0.001$ versus control.
AP: Apatite; C: Control; LPS: Lipopolysaccharide; Pg: Peptidoglycan; Sol: Soluble.

this is bypassed, such as with intravenous (iv.) infusion (e.g., iv. iron oxide nanoparticles) or intradermal injection (e.g., with tattoo ink), there is adequate circulation of particles and cells to ensure health of the organism and local structures despite marked particle-loading of cells. However, *in vitro*, one ensures that cell loading with particles matches a potential *in vivo* situation is not easily addressed. However, gorging to the point of cell dysfunction or even death is unlikely to represent 'real life'. Genuinely toxic particles ought to be seen as such without the need for cells to gorge excessively and abnormally.

Finally, while our data suggest that apatitic nanoparticles do not stimulate inflammasome activation or, therefore, IL-1β secretion even in the presence of a proinflammatory stimulus, this need not apply to all (nano)particles. For example, α-quartz silica particles are toxic: they are proinflammatory and fibrogenic *in vivo* and their genuine role in inflammasome activation seems most likely [6,42,43]. Amorphous microparticles of silica appear relatively benign; however, as they decrease in size into the 'nano' range, they adopt some of the inflammatory characteristics of their α-quartz crystalline counterpart [44]. Fine nanoparticulate silica may therefore also activate the inflammasome. There may well be others but, nonetheless, our data challenge the idea that nanoparticles/nanominerals are necessarily special activators of the inflammasome.

Conclusion

In vitro investigation of nanoparticles/nanominerals and their potential role in the inflammasome axis requires careful experimental consideration as artefactual activation may ensue under certain conditions and therefore lead to misinterpretation. Future work should consider them carefully on a case-by-case basis, as we have done here for apatitic nanoparticles.

Future perspective

We anticipate that relatively few nanomaterials will be shown to activate the inflammasome *per se* and probably in numbers not outstanding from their coarse microparticle and microfibre counterparts (e.g., quartz, asbestos). The fact that nanoparticles may act as vehicles to introduce adsorbed or entrapped substrate into cells, which in turn could activate the inflammasome, is not to be disputed. We also anticipate much greater scientific scrutiny to be given over to conditions of particle loading and experimental design in cellular or animal models that seek to understand toxicity and/or cellular handling of nanomaterials for 'real life' scenarios. We expect the arbitrary cut off of 100 nm as a nano-definition to be redundant and that the 'nano' term will be used in disciplines depending on relevant behavioral and functional activities. For example, biologically it is the mechanism of uptake and thereafter the cellular compartment that is first engaged that separates a 'nano' particle from a 'micro' particle. Finally and as previously stated by our group [2], we expect that nanoforms will be understood as safe, naturally occurring and of physiological benefit under some circumstances.

Acknowledgements

The authors wish to thank Benjamin Harris for carrying out the assessment of calcium phosphate toxicity, Vinay Thoree for the preparation of calcium phosphate for downstream characterization and Jack Robertson for undertaking infrared analyses.

Financial & competing interests disclosure

The authors thank UK Medical Research Council (Grant number U105960399) for their continued support. The

authors have no other relevant affiliations or financial involvement with any organization or entity with a financial interest in or financial conflict with the subject matter or materials discussed in the manuscript apart from those disclosed.

No writing assistance was utilized in the production of this manuscript.

Ethical conduct of research

The authors state that they have obtained appropriate institutional review board approval or have followed the principles outlined in the Declaration of Helsinki for all human or animal experimental investigations. In addition, for investigations involving human subjects, informed consent has been obtained from the participants involved.

Executive summary

- Discrepancies in the role of (nano)particles in inflammasome activation *in vivo* and *in vitro* have been noted, suggesting that applied *in vitro* experimental conditions do not always adequately mimic *in vivo* situations.
- Here, calcium phosphate (apatite) nanoparticles were synthesized *in situ* and ensuing caspase1/IL-1β cellular responses studied in peripheral blood mononuclear cells, under different *in vitro* conditions.
- Caspase 1/IL-1β responses to apatitic nanoparticles were strongly influenced by the purity of starting material (i.e., attenuated in aseptic conditions), resting status of cells (i.e., nonexistent in experiments using rested cells), and duration of particle exposure (unavoidably triggered by abnormally prolonged incubation).
- This work clearly highlights that, in addition to particle characteristics, it is necessary to carefully establish experimental conditions when studying *in vitro* cellular responses to nanoparticles, as artefactual activation may ensue.

References

Papers of special note have been highlighted as:
• of interest

1 Nel AE, Madler L, Velegol D *et al*. Understanding biophysicochemical interactions at the nano-bio interface. *Nat. Mater.* 8(7), 543–557 (2009).

• **Comprehensive review on the physicochemical factors that shape nanoparticle–cell interactions in biological surroundings.**

2 Powell JJ, Faria N, Thomas-McKay E, Pele LC. Origin and fate of dietary nanoparticles and microparticles in the gastrointestinal tract. *J. Autoimmun.* 34(3), 226–233 (2010).

• **Comprehensive review of the 'bear traps' in nanomineral characterization, definition and attribution of biological properties.**

3 Monopoli MP, Aberg C, Salvati A, Dawson KA. Biomolecular coronas provide the biological identity of nanosized materials. *Nat. Nanotechnol.* 7(12), 779–786 (2012).

• **Emphasizes the importance of the particle corona in dictating its biological outcome.**

4 Martinon F, Petrilli V, Mayor A, Tardivel A, Tschopp J. Gout-associated uric acid crystals activate the NALP3 inflammasome. *Nature* 440(7081), 237–241 (2006).

• **Seminal work that set the scene in particle and inflammasome research.**

5 Demento SL, Eisenbarth SC, Foellmer HG *et al*. Inflammasome-activating nanoparticles as modular systems for optimizing vaccine efficacy. *Vaccine* 27(23), 3013–3021 (2009).

6 Dostert C, Petrilli V, Van Bruggen R, Steele C, Mossman BT, Tschopp J. Innate immune activation through Nalp3 inflammasome sensing of asbestos and silica. *Science* 320(5876), 674–677 (2008).

7 Peng HH, Wu CY, Young D *et al*. Physicochemical and biological properties of biomimetic mineralo-protein nanoparticles formed spontaneously in biological fluids. *Small* 9(13), 2297–2307 (2013).

8 Rock KL, Kataoka H, Lai JJ. Uric acid as a danger signal in gout and its comorbidities. *Nat. Rev. Rheumatol.* 9(1), 13–23 (2013).

9 Vaine CA, Patel MK, Zhu J *et al*. Tuning innate immune activation by surface texturing of polymer microparticles: the role of shape in inflammasome activation. *J. Immunol.* 190(7), 3525–3532 (2013).

10 Winter M, Beer HD, Hornung V, Kramer U, Schins RP, Forster I. Activation of the inflammasome by amorphous silica and TiO_2 nanoparticles in murine dendritic cells. *Nanotoxicology* 5(3), 326–340 (2011).

11 Latz E, Xiao TS, Stutz A. Activation and regulation of the inflammasomes. *Nat. Rev. Immunol.* 13(6), 397–411 (2013).

• **Up-to-date and elegant review on the inflammasome family.**

12 Franchi L, Eigenbrod T, Munoz-Planillo R, Nunez G. The inflammasome: a caspase-1-activation platform that regulates immune responses and disease pathogenesis. *Nat. Immunol.* 10(3), 241–247 (2009).

13 Dorozhkin SV. Bioceramics of calcium orthophosphates. *Biomaterials* 31(7), 1465–1485 (2010).

14 Ea HK, Chobaz V, Nguyen C *et al*. Pathogenic role of basic calcium phosphate crystals in destructive arthropathies. *PLoS ONE* 8(2), e57352 (2013).

15 Jin C, Frayssinet P, Pelker R *et al*. NLRP3 inflammasome plays a critical role in the pathogenesis of hydroxyapatite-associated arthropathy. *Proc. Natl Acad. Sci. USA* 108(36), 14867–14872 (2011).

16 Pazar B, Ea HK, Narayan S *et al*. Basic calcium phosphate crystals induce monocyte/macrophage IL-1beta secretion through the NLRP3 inflammasome *in vitro*. *J. Immunol.* 186(4), 2495–2502 (2011).

17 Evans SM, Ashwood P, Warley A, Berisha F, Thompson RP, Powell JJ. The role of dietary microparticles and calcium in apoptosis and interleukin-1beta release of intestinal macrophages. *Gastroenterology* 123(5), 1543–1553 (2002).

18 Dinarello CA. Immunological and inflammatory functions of the interleukin-1 family. *Annu. Rev. Immunol.* 27, 519–550 (2009).

19 Juhasz JA, Best SM, Auffret AD, Bonfield W. Biological control of apatite growth in simulated body fluid and human blood serum. *J. Mater. Sci. Mater. Med.* 19(4), 1823–1829 (2008).

20 Gustavsson J, Ginebra MP, Engel E, Planell J. Ion reactivity of calcium-deficient hydroxyapatite in standard cell culture media. *Acta Biomater.* 7(12), 4242–4252 (2011).

21 Bilton M, Milne SJ, Brown AP. Comparison of hydrothermal and sol-gel synthesis of nano-particulate hydroxyapatite by characterisation at the bulk and particle level. *Open J. Inorgan. Nonmetallic Materials* 2(1), 1–10 (2012).

22 Van Der Houwen JaM, Cressey G, Cressey BA, Valsami-Jones E. The effect of organic ligands on the crystallinity of calcium phosphate. *J. Cryst. Growth* 249(3–4), 572–583 (2003).

23 Berry EE, Leach SA. The structure of some calcium deficient apatites. *Arch. Oral Biol.* 12(1), 171–174 (1967).

24 Raynaud S, Champion E, Bernache-Assollant D, Thomas P. Calcium phosphate apatites with variable Ca/P atomic ratio I. Synthesis, characterisation and thermal stability of powders. *Biomaterials* 23(4), 1065–1072 (2002).

25 Cassel SL, Sutterwala FS. Sterile inflammatory responses mediated by the NLRP3 inflammasome. *Eur. J. Immunol.* 40(3), 607–611 (2010).

26 Fleshner M. Stress-evoked sterile inflammation, danger associated molecular patterns (DAMPs), microbial associated molecular patterns (MAMPs) and the inflammasome. *Brain Behav. Immun.* 27(1), 1–7 (2013).

27 Galliher-Beckley AJ, Lan LQ, Aono S, Wang L, Shi J. Caspase-1 activation and mature interleukin-1beta release are uncoupled events in monocytes. *World J. Biol. Chem.* 4(2), 30–34 (2013).

28 Laliberte RE, Perregaux DG, McNiff P, Gabel CA. Human monocyte ATP-induced IL-1 beta posttranslational processing is a dynamic process dependent on *in vitro* growth conditions. *J. Leukoc. Biol.* 62(2), 227–239 (1997).

29 Netea MG, Nold-Petry CA, Nold MF *et al*. Differential requirement for the activation of the inflammasome for processing and release of IL-1beta in monocytes and macrophages.. *Blood* 113(10), 2324–2335 (2009).

30 Moghimi SM, Andersen AJ, Ahmadvand D, Wibroe PP, Andresen TL, Hunter AC. Material properties in complement activation. *Adv. Drug Deliv. Rev.* 63(12), 1000–1007 (2011).

31 Laudisi F, Spreafico R, Evrard M *et al*. Cutting edge: the NLRP3 inflammasome links complement-mediated inflammation and IL-1beta release. *J. Immunol.* 191(3), 1006–1010 (2011).

32 Caicedo MS, Samelko L, McAllister K, Jacobs JJ, Hallab NJ. Increasing both CoCrMo-alloy particle size and surface irregularity induces increased macrophage inflammasome activation *in vitro* potentially through lysosomal destabilization mechanisms. *J. Orthop. Res.* 31(10), 1633–1642 (2013).

33 Morishige T, Yoshioka Y, Inakura H *et al*. The effect of surface modification of amorphous silica particles on NLRP3 inflammasome mediated IL-1beta production, ROS production and endosomal rupture. *Biomaterials* 31(26), 6833–6842 (2010).

34 Morishige T, Yoshioka Y, Tanabe A *et al*. Titanium dioxide induces different levels of IL-1beta production dependent on its particle characteristics through caspase-1 activation mediated by reactive oxygen species and cathepsin B. *Biochem. Biophys. Res Commun.* 392(2), 160–165 (2010).

35 Mahamid J, Sharir A, Gur D, Zelzer E, Addadi L, Weiner S. Bone mineralization proceeds through intracellular calcium phosphate loaded vesicles: a cryo-electron microscopy study. *J. Struct. Biol.* 174(3), 527–535 (2011).

36 Wang YH, Liu Y, Maye P, Rowe DW. Examination of mineralized nodule formation in living osteoblastic cultures using fluorescent dyes. *Biotechnol. Prog.* 22(6), 1697–1701 (2006).

37 Asong J, Wolfert MA, Maiti KK, Miller D, Boons GJ. Binding and cellular activation studies reveal that Toll-like receptor 2 can differentially recognize peptidoglycan from Gram-positive and Gram-negative bacteria. *J. Biol. Chem.* 284(13), 8643–8653 (2009).

38 Hewitt RE, Pele LC, Tremelling M, Metz A, Parkes M, Powell JJ. Immuno-inhibitory PD-L1 can be induced by a peptidoglycan/NOD2 mediated pathway in primary monocytic cells and is deficient in Crohn's patients with homozygous NOD2 mutations. *Clin. Immunol.* 143(2), 162–169 (2012).

39 Iyer JK, Coggeshall KM. Cutting edge: primary innate immune cells respond efficiently to polymeric peptidoglycan, but not to peptidoglycan monomers. *J. Immunol.* 186(7), 3841–3845 (2011).

40 Narayan S, Pazar B, Ea HK *et al*. Octacalcium phosphate crystals induce inflammation *in vivo* through interleukin-1 but independent of the NLRP3 inflammasome in mice. *Arthritis Rheum.* 63(2), 422–433 (2011).

41 Smythies LE, Sellers M, Clements RH *et al*. Human intestinal macrophages display profound inflammatory anergy despite avid phagocytic and bacteriocidal activity. *J. Clin. Invest.* 115(1), 66–75 (2005).

42 Cassel SL, Eisenbarth SC, Iyer SS *et al*. The Nalp3 inflammasome is essential for the development of silicosis. *Proc. Natl Acad. Sci. USA* 105(26), 9035–9040 (2008).

43 Hornung V, Bauernfeind F, Halle A *et al*. Silica crystals and aluminium salts activate the NALP3 inflammasome through phagosomal destabilization. *Nat. Immunol.* 9(8), 847–856 (2008).

44 Sandberg WJ, Lag M, Holme JA *et al*. Comparison of non-crystalline silica nanoparticles in IL-1beta release from macrophages. *Part. Fibre Toxicol.* 9, 32 (2012).